Settling of heated inertial particles through homogeneous turbulence

By A. Frankel, H. Pouransari, F. Coletti† AND A. Mani

Particle-laden flows in which the dispersed phase is not isothermal with the continuous phase are common in a wealth of natural and industrial settings. In this study we consider the case of inertial particles heated by thermal radiation while settling through a turbulent transparent gas. Numerical simulations of forced turbulence are performed in which the two-way coupling between dispersed and continuous phase is taken into account. The momentum and energy equations are solved in a triply periodic domain with the point particle model. Solid particles of different densities and much smaller than the smallest flow scales are considered. We consider dilute and optically thin regimes in which each particle receives the same heat flux. The particle Stokes number (based on the Kolmogorov time scale) is of order unity, which causes strong preferential concentration. The nominal settling velocity is of the same order as the Kolmogorov velocity for the lighter particles, but an order of magnitude larger for the heavier particles. Even though the volume fraction is relatively low, the mass loading is sufficiently large for the particle phase to affect the turbulence even in the absence of radiation. Specifically, it is found that non-heated particles enhance turbulence when their settling velocity is sufficiently high. When heated, particles shed plumes of buoyant gas, further modifying the turbulence structure and increasing velocity fluctuations in the vertical direction. For the lighter particles, this also causes a substantial reduction of the mean settling velocity. The radiative forcing does not affect preferential concentration, but eliminates preferential sweeping: the heated particles do not sample regions of downward fluid motion.

1. Introduction

For particles much denser than the carrier fluid and small compared to the flow scales, the relevant parameter describing the particle-fluid interaction is the Stokes number $\mathrm{St} = \tau_p/\tau_f$, the ratio between the aerodynamic response time of the particle and the fluid time scale. When the latter is taken as the Kolmogorov scale τ_η, the maximum level of preferential concentration is typically found at $\mathrm{St}_\eta \approx 1$, where the clustering is driven by the small and intense turbulent fluctuations. In the last decades the use of advanced experimental and numerical approaches has allowed understanding of the origin of particles clustering in turbulent flows (Eaton & Fessler 1994) and their consequences on the statistics of particle motion (Bec *et al.* 2006) and on their collision rate (Sundaram & Collins 1997).

Compared to the clustering of particles in turbulence, the dynamics of gravitational settling of inertial particles through turbulence has received less attention, despite their strong practical relevance. Turbulence can increase the settling velocity of small inertial particles beyond their nominal terminal velocity V_t that they would have in a quiescent fluid because trajectories that sample the downward side of the eddies are favored. This

† Department of Aerospace Engineering and Mechanics, University of Minnesota

mechanism, referred to as preferential sweeping, has been first demonstrated in homogeneous isotropic turbulence by Wang & Maxey (1993). Measurements from Aliseda *et al.* (2002) and Yang & Shy (2005) confirmed this effect, which is especially strong when $\mathrm{St}_\eta \approx 1$ and $V_t/u' \approx 0.5$, u' being the rms fluid velocity fluctuation (Dejoan & Monchaux 2013). Depending on which turbulent scales are considered crucial for the settling rate (the large eddies of characteristic velocity u' rather than the Kolmogorov size eddies of characteristic velocity u_η), researchers have used the ratios V_t/u' or V_t/u_η (Yang & Lei 1998). V_t/u_η is sometimes referred to as the settling parameter.

If the loading is sufficiently high or the particle size is not small compared to the smallest flow scales, a two-way coupled regime will set in. In particular, turbulence will be either enhanced or reduced depending on the particle size, Stokes number, and loading (see the review by Balachandar & Eaton 2010). For particles of diameter D_p much smaller than the Kolmogorov scale η and Stokes number $\mathrm{St}_\eta \approx 1$, studies in both homogenous and sheared turbulent flows are consistent in showing a global decrease of turbulence, with depletion of turbulent energy at large scales and injection at small scales (Elghobashi & Truesdell 1993; Poelma *et al.* 2007).

When gravity acts on a two-way coupled dispersed flow, the breaking of symmetry causes anisotropy in otherwise isotropic or even quiescent environments. Heavy particles settling through turbulence may exert a non-negligible collective drag on the carrier fluid, which adds to the preferential sweeping and increases the settling rate (Bosse *et al.* 2006), while the turbulent energy is redistributed from the horizontal to the vertical direction (Ferrante & Elghobashi 2003). In the absence of hydrodynamic forcing, velocity fluctuations in the fluids will be solely caused by the momentum coupling with the settling particles. The induced eddies can span a wide spectrum of scales due to the formation of large clusters (Capecelatro *et al.* 2014). Similarly, rising bubbles induce anisotropic turbulence in the liquid phase (so-called pseudo-turbulence), with higher energy content in the vertical direction (Bunner & Tryggvason 2002). Recently we have shown that, in an otherwise stagnant particle-gas mixture, the radiative heating of particles can result in the formation of buoyant plumes and highly intermittent concentration, leading to a turbulent state sustained only by the radiation (Zamansky *et al.* 2014).

In the present study we explore the behavior of heated particles settling through externally driven homogeneous turbulence, and the interaction between dispersed and continuous phases. The physical parameters are chosen to be representative of a diluted, optically thin mixture of air and solid particles subject to thermal radiation. Numerical simulations are performed taking into account the two-way coupling of both momentum and temperature between dispersed and continuous phase. Since particles much smaller than the smallest flow scales are considered, all relevant spatio-temporal scales can be resolved. The particle Stokes number and settling velocity are chosen to produce significant preferential concentration. While settling, the clustered particles shed plumes of buoyant fluid modifying the turbulence structure, which in turn alters both the concentration field and the settling rate. Such phenomena have not been investigated before.

2. Methodology

2.1. *Governing equations*

The compressible low-Mach Navier-Stokes equation for a fluid of constant viscosity μ is

$$\frac{\partial \rho}{\partial t} + \frac{\partial \rho u_j}{\partial x_j} = 0 \tag{2.1}$$

$$\frac{\partial \rho u_i}{\partial t} + \frac{\partial \rho u_i u_j}{\partial x_j} = -\frac{\partial p}{\partial x_i} + \frac{\partial \tau_{ij}}{\partial x_j} + \rho g_i - \sum_{n=1}^{N_p} \frac{m_p}{\tau_p}(u_i - v_{i,n})\delta(x_i - y_{i,n}), \tag{2.2}$$

where u_i are the velocity components, t is time, x_i are the spatial coordinates, p is the hydrodynamic pressure, τ_{ij} is the Newtonian viscous stress tensor, ρ is the fluid density, g_i $(i = 3)$ is the gravitational acceleration, δ_{ij} is the Kronecker delta, N_p is the number of particles in an Eulerian cell, and $v_{i,n}$ and $y_{i,n}$ are the velocity and spatial coordinates of the n-th particle. Though the domain is triply periodic, the addition of gravity renders the vertical direction asymmetric with respect to the two horizontal directions. Because we consider spherical Stokesian particles, their mass and aerodynamic response time are $m_p = \rho_p \pi D_p^3/6$ and $\tau_p = \rho_p D_p^2/18\mu$, respectively, ρ_p being the particle density. The fluid is considered to be an ideal gas of constant thermal conductivity k and heat capacities C_v and C_p (at constant volume and pressure, respectively), for which the energy equation reads

$$\frac{\partial}{\partial t}(\rho C_v T_f) + \frac{\partial}{\partial x_j}(\rho C_p T_f u_j) = k\frac{\partial^2 T_f}{\partial x_j \partial x_j} + \sum_{n=1}^{N_p} \pi D_p^2 h(T_{p,n} - T_f)\delta(x_i - y_{i,n}), \tag{2.3}$$

where T_f is the fluid temperature, $T_{p,n}$ is the temperature of the n-th particle and h is the convective heat transfer coefficient, which for a Stokesian particle can be calculated from the Nusselt number $\mathrm{Nu} = hD_p/k = 2$. The gas properties reflect those of air at ambient temperature and pressure.

Particles are individually tracked along their trajectories, according to the simplified particle equation of motion, where only contributions from Stokes drag and gravity are retained,

$$\frac{dy_i}{dt} = v_i \qquad \frac{dv_i}{dt} = \frac{u_i - v_i}{\tau_p} + g_i. \tag{2.4}$$

Under the Stokesian particle assumption, the terminal velocity of the particles is $V_t = g\tau_p$. The particles are subject to a thermal radiation of heat flux I_o. The carrier phase is transparent to radiation, whereas the incident radiative flux on each particle is completely absorbed. Because we focus on relatively small volume fractions, the fluid-particle medium is considered optically thin. Under these hypotheses, the direction of the radiation is inconsequential, each particle receives the same radiative heat flux, and its temperature T_p is governed by

$$\frac{d}{dt}(m_p C_{v,p} T_p) = \frac{\pi D_p^2}{4} I_o - \pi D_p^2 h(T_p - T_f) \tag{2.5}$$

where $C_{v,p}$ is the particle specific heat.

2.2. *Numerical implementation*

Each of the above equations is solved in an Eulerian framework using a staggered grid formulation and second-order central differences. The pressure Poisson equation is solved with a spectral method, and both the fluid and particle equations are integrated in time using a fourth order Runge-Kutta time integrator. Eulerian quantities are evaluated at the location of the particles using linear interpolation, and coupling from the particle to the fluid is performed with linear projection to the nearest fluid volumes. The initial conditions for the simulations are generated from a Passot-Pouquet spectrum with the particles distributed randomly throughout the computational domain. The turbulence is maintained using a linear forcing method (Rosales & Meneveau 2005). The domain is a triply periodic cube of size $L_b = 0.237$m, which is discretized in N^3 points such

that the Kolmogorov scales are resolved ($L_b/N = \Delta < \eta$). For the one-way coupled simulation without radiation, in which the flow scales are predicted by homogeneous isotropic turbulence theory, $N = 256$. For the cases in which two-way coupling and radiation enhances the turbulence agitation (and so reduces the the Kolmogorov length), N is increased accordingly. The fluid is considered an ideal gas, with constant dynamic viscosity $\mu = 1.9 \times 10^{-5}\,\mathrm{Pa \cdot s}$, and an initial density of $\rho_o = 1.2\ \mathrm{kg/m^3}$ at a temperature of $T_o = 300\mathrm{K}$. The mean fluid momentum is set to zero in each time step, which is equivalent to applying a mean hydrostatic pressure gradient to the fluid. This is necessary to prevent the fluid from accelerating continuously in vertical direction, due to the drag imposed by the settling particles and by the buoyancy (Maxey & Patel 2001; Bosse *et al.* 2005). Similarly, the mean temperature of the fluid is artificially set to be constant, to prevent the fluid from warming up indefinitely. Therefore the velocity and temperature dynamics investigated in this study have to be considered fluctuations around a potentially time-varying mean. This approach allows us to focus on the fundamental aspects of the turbulent particle-laden flow.

2.3. *Physical Parameters*

The main parameters describing the turbulent fluid phase and the dispersed particle phase for the performed simulations are listed in Table 1. The values are representative of the system after it has become stationary (typically after two or three eddy turnover times). A total of ten cases are considered. Three particle material densities (ρ_p between 1000 and 10000 $\mathrm{kg/m^3}$) and three radiation intensity levels (I_o between 0 and 2 $\mathrm{MW/m^2}$) are considered. A baseline case with no radiation and one-way coupled particle transport is considered for comparison. Because of the anisotropy caused by the multi-way coupling, we define as the velocity and length scale of the large eddies, respectively, $u' = \sqrt{2\mathrm{TKE}/3} = \sqrt{2u_{rms}^2/3 + w_{rms}^2/3}$ and $L = u'^3/\epsilon$ where $\mathrm{TKE} = 0.5(2u_{rms}^2 + w_{rms}^2)$ is the turbulent kinetic energy, u_{rms} and w_{rms} are the rms fluctuations of the horizontal and vertical components, and ϵ is the turbulent dissipation rate. Note that it has been assumed that the two horizontal components are identical in the above formulas. The hydrodynamic forcing parameter is the same for all cases, and produces a microscale Reynolds number $\mathrm{Re}_{\lambda,\Phi_v=0} = 65$ in the one-way coupled regime (where $\Phi_v = 0$ subscript denotes no mass loading). In every case the particle diameter is assumed to be $D_p = 40\,\mu\mathrm{m}$, which results in $D_p/\eta \leq 0.1$ and $\mathrm{Re}_p \leq 1$, confirming the validity of the point-particle approximation. On the other hand, the volume fraction is $\Phi_v = 10^{-5}$ (corresponding to a mass fraction Φ_m between 1% and 10%), which is considered in the two-way coupled regime. The momentum transfer from the heavy particles and the buoyancy-driven plumes strongly modify the turbulence structure, as evident for example from the changes in the Re_λ between the various cases. The change in turbulent scales also alters the effective Stokes number and the settling parameter. The St_η values studied are consistent with the occurrence of strong preferential concentration effects. The level of radiation is associated with a steady state particle temperature increase with respect to the surrounding fluid. From Eq. (2.5), this temperature increase is $T_p - T_o = D_p I_o/8k$ where $\mathrm{Nu} = hD_p/k = 2$ has been substituted, which is valid for spherical particles at the present Re_p range. The particle-to-fluid temperature ratio is 1.3 for the intermediate and 2.2 for the higher radiation level.

	One-way	Two-way								
	No radiation				Radiation					
Run #	0	1	2	3	4	5	6	7	8	9
I[MW/m^2]	0	0	0	0	0.5	0.5	0.5	2	2	2
ρ_p[kg/m^3]	1000	1000	5000	10000	1000	5000	10000	1000	5000	10000
L_e[mm]	40.1	38.5	63.9	88.2	40.0	56.8	76.8	31.0	52.1	68.4
λ[mm]	10.5	10.0	9.8	9.7	9.0	9.6	9.9	7.2	7.6	8.3
η[mm]	0.64	0.66	0.48	0.37	0.57	0.5	0.48	0.43	0.37	0.36
T_e[ms]	409	414	356	303	345	353	389	205	223	246
τ_η[ms]	26.0	27.5	14.1	8.8	20.1	15.4	14.2	11.9	8.6	8.0
u'[m/s]	0.098	0.093	0.17	0.25	0.17	0.15	0.18	0.15	0.22	0.25
u_η[m/s]	0.025	0.024	0.034	0.043	0.028	0.032	0.033	0.036	0.043	0.044
ϵ[m^2/s^3]	0.024	0.021	0.079	0.21	0.039	0.066	0.079	0.11	0.22	0.25
τ_p[ms]	4.7	4.7	23.4	46.8	4.7	23.4	46.8	4.7	23.4	46.8
V_t[m/s]	0.046	0.046	0.23	0.46	0.046	0.23	0.46	0.046	0.23	0.46
ρ_p/ρ_o	833	833	4166	8333	833	4166	8333	833	4166	8333
Φ_m	0.01	0.01	0.05	0.1	0.01	0.05	0.1	0.01	0.05	0.1
Re_λ	65	59	104	153	66	93	109	69	105	129
St_η	0.18	0.17	1.6	5.1	0.23	1.48	3.4	0.39	2.7	5.8
V_t/u'	0.47	0.49	1.37	1.84	0.40	1.50	2.62	0.30	1.05	1.87
V_t/u_η	1.84	1.91	6.75	10.68	1.64	7.17	13.91	1.28	5.34	10.43
T_p/T_o	1	1	1	1	1.3	1.3	1.3	2.21	2.21	2.21

TABLE 1. Summary of the simulation parameters and turbulence statistics for each of the mass loadings and radiation heat fluxes.

3. Results

3.1. *Turbulent flow characteristics*

3.1.1. *Settling without radiation*

When gravitational settling is not a dominant effect (i.e. $V_t/u' \ll 1$), small inertial particles are known to reduce the kinetic energy and dissipation in a two-way coupled system. Here we consider particles of significant settling velocities compared to both the small- and large-scale turbulent velocity, and we find that turbulent agitation is enhanced by the faster settling particles. This is clearly illustrated in Figure 1, that displays values of TKE and ϵ normalized by their correspondent levels in the one-way coupled (effectively unladen) case, $\mathrm{TKE}_{\Phi=0}$ and $\epsilon_{\Phi=0}$. For $\rho_p/\rho_o = 833$, which corresponds to settling velocities of the same order as the turbulent velocity scales (see Table 1), the turbulent energy and dissipation rate are slightly smaller than those in the one-way coupled flow, in agreement with previous findings (Bosse *et al.* 2006). However, for heavier particles with settling parameters $V_t/u_\eta = \mathcal{O}(10)$, both TKE and ϵ increase greatly. This effect cannot be attributed to the loading since the turbulent energy has been shown to decrease with increasing mass loading (Squires & Eaton 1990; Boivin *et al.* 1998). The cause is rather to be found in the drag force exerted by the quickly setting particles, which alters the flow structure. When a particle falls, the lost gravitational potential energy is an input of kinetic energy into the fluid. This is observed in the enhancement of vertical velocity fluctuations with respect to the horizontal fluctuations, represented by the w_{rms}/u_{rms} ratio plotted in Figure 2, which exceeds 2 for the $\rho_p/\rho_o = 8333$ case (corresponding to

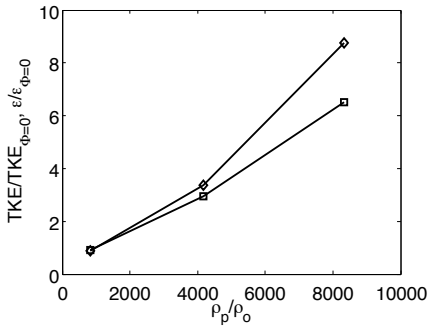

FIGURE 1. Dependence of the TKE (□) and dissipation (◇) on particle bulk density of the two-way coupled simulations relative to a one-way coupled simulation. The increased TKE and dissipation at higher mass loading indicates the transfer of gravitational potential energy from the particles to the surrounding fluid.

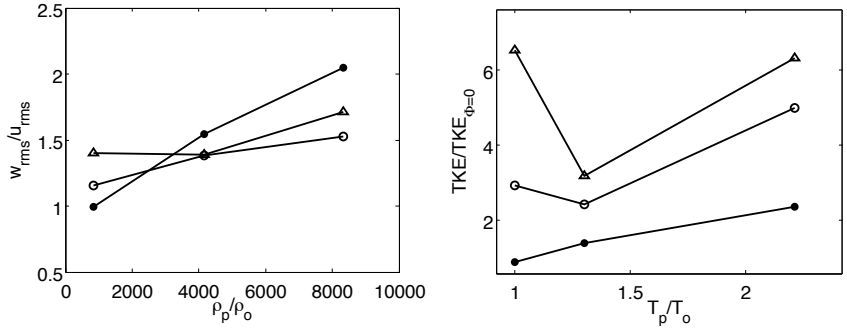

FIGURE 2. The ratio of the root-mean-square fluctuations of vertical to horizontal velocity in the fluid for each of the different particle densities and temperatures (left, • : $T_p/T_o = 1$, ○ : $T_p/T_o = 1.3$, △ : $T_p/T_o = 2.2$) and the total TKE in each simulation (right, • : $\rho_p/\rho_o = 833$, ○ : $\rho_p/\rho_o = 4166$, △ : $\rho_p/\rho_o = 8333$).

$V_t/u_\eta = 10.68$). Therefore, rapidly settling particles, in the absence of radiation, promote turbulence and cause strong anisotropy.

3.1.2. *Settling with radiation*

In the presence of relatively light particles, the radiative heating causes a substantial increase in turbulent agitation, especially in terms of vertical velocity fluctuations. The violent vertical flow motions are caused by hot particles releasing heat and therefore generating buoyant plumes, especially at the locations where they cluster. This is consistent with the increasingly high values of w_{rms}/u_{rms} for higher particle temperature, as reported in Figure 2 at $\rho_p/\rho_o = 833$.

On the other hand, for heavier particles ($\rho_p/\rho_o = 4166$ and 8333) Figure 2 indicates that the anisotropy is reduced by the radiative heating. This behavior may seem contradictory, because one expects the buoyant plumes of heated gas to promote stronger vertical velocity fluctuations and increase turbulence production. Radiation and gravitation inject momentum into the career fluid in opposite directions (respectively upward and downward). Therefore, it is natural to expect some cancelation on the effects of the two phenomena on the induced turbulence.

As further proof of this behavior, Figure 2 presents plots of TKE/TKE$_{\Phi=0}$ as a function

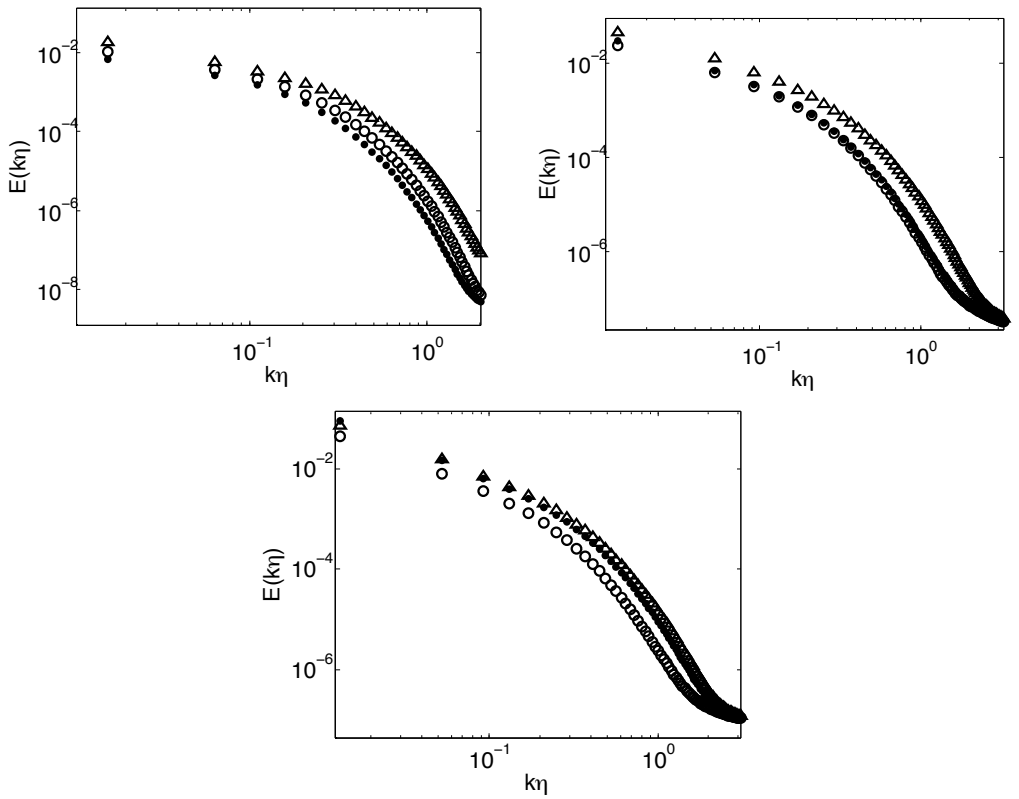

FIGURE 3. Turbulent energy wavenumber spectra for each of the particle temperatures ($\bullet$: $T_p/T_o = 1$, $\circ$: $T_p/T_o = 1.3$, $\triangle$: $T_p/T_o = 2.2$) at $\rho_p/\rho_o = 833$ (top left), 4166 (top right), and 8333 (bottom).

of the particle temperature, for the considered density ratios. For $\rho_p/\rho_o > 833$, at intermediate radiation intensity the turbulent kinetic energy is reduced with respect to the non-radiative case. Only at the highest radiation level the increase in buoyancy-related production offsets the drop in turbulent energy caused by the hindered settling. The energy spectra provide information on the scales at which the momentum coupling and the radiation-induced buoyancy act. For the relatively light particles ($\rho_p/\rho_o = 833$, Figure 3), a small spike in the spectrum is visible at high wavenumbers, which corresponds to the energy injected by the particles at small scales. Heating the particles produces a strong increase of energy, especially at small scales, due to the local plumes. For heavier particles, the spike at high wavenumbers is much more pronounced, and is almost unaffected by the thermal radiation. The increase or decrease in turbulent energy with radiation (summarized in Figure 2) happens rather at intermediate and large scales.

3.2. *Particle settling*

Figure 4 shows the fractional difference of the mean settling velocity W_p (in absolute value) with respect to the nominal settling velocity V_t. In absence of radiation, the settling velocity is 22% to 35% higher than the terminal velocity. This is due to both preferential sweeping by the turbulent eddies (Wang & Maxey 1993), and the drag exerted on the fluid by the particles (Bosse *et al.* 2006). These values are in general agreement with

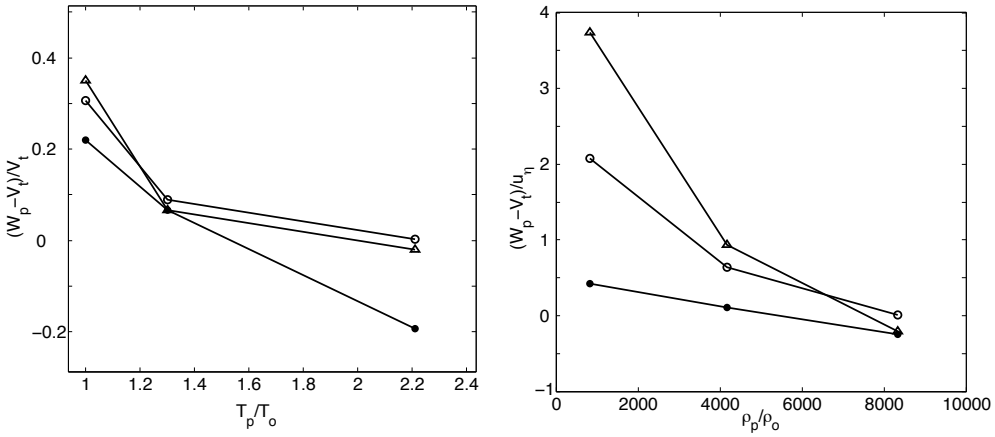

FIGURE 4. The relative difference in the mean particle settling velocity and the terminal velocity of the particles in a quiescent fluid, normalized by the particle terminal velocity (left, $\bullet$: $T_p/T_o = 1$, $\circ$: $T_p/T_o = 1.3$, $\triangle$: $T_p/T_o = 2.2$) and the Kolmogorov velocity (right, $\bullet$: $\rho_p/\rho_o = 833$, $\circ$: $\rho_p/\rho_o = 4166$, $\triangle$: $\rho_p/\rho_o = 8333$). As the particles are heated, the relative settling velocity decreases.

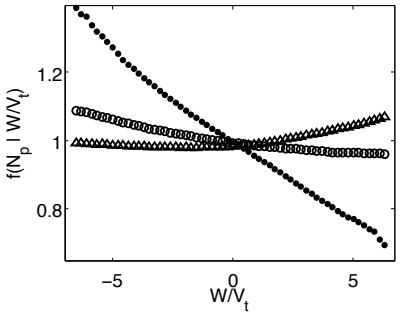

FIGURE 5. The probability density function for the concentration of particles conditioned on local fluid velocity for $\rho_p/\rho_o = 833$ at different temperatures ($\bullet$: $T_p/T_o = 1$, $\circ$: $T_p/T_o = 1.3$, $\triangle$: $T_p/T_o = 2.2$). The addition of radiation biases the concentration of particles towards regions of upward fluid motion.

the literature, although for the denser particles, we are in a regime of higher settling parameter than reported before.

In the presence of radiative heating, the hot particles heat up the air around them, and the locally buoyant air tends to retard their fall, as apparent in Figure 4 for $T_p/T_o > 1$. We remark that this behavior is not the consequence of a global upward fluid velocity (since the mean fluid velocity is set to zero at every time step), but the product of localized heating. The preferential sweeping mechanism, which is expected to occur for the particles at $\rho_p/\rho_o = 833$, which have both Stokes number and settling parameters of order unity, is clearly not effective in the radiative regime. This is confirmed by Figure 5, where the number density of particles is plotted as a function of the local vertical fluid velocity, for the cases at zero and intermediate radiation. Without radiation, as expected, particles tend to concentrate in regions of downward velocity (Wang & Maxey 1993). This effect is practically absent in the presence of radiation.

From Figure 4 it is also evident that the hindering of the settling velocity is much

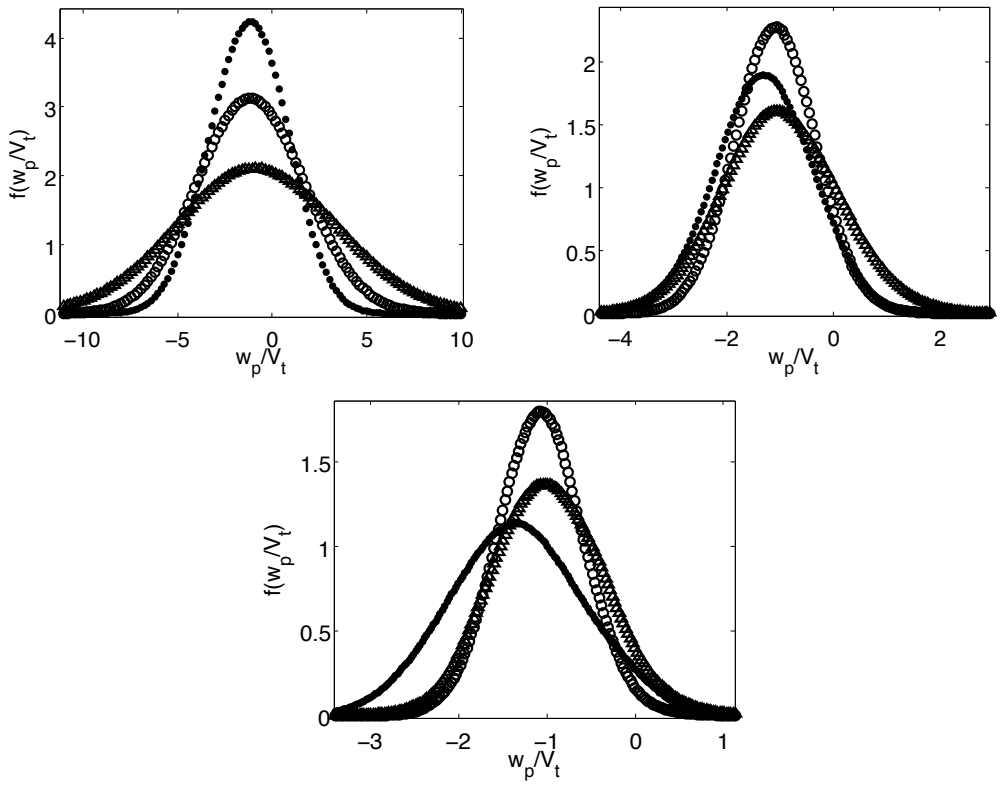

FIGURE 6. Probability density functions of particle vertical velocity for each of the particle temperatures ($\bullet : T_p/T_o = 1$, $\circ : T_p/T_o = 1.3$, $\triangle : T_p/T_o = 2.2$) at $\rho_p/\rho_o = 833$ (top left), 4166 (top right), and 8333 (bottom).

stronger for lighter particles. This is likely caused by the fact that the faster falling particles are quickly decoupled from the upward buoyant plumes, and so are less influenced by the upward draft motion of the fluid they heat. Even though the fractional change in settling velocity is less pronounced for heavy particles, its impact on the particle-turbulence interaction is potentially large. This is suggested by Figure 4, where the reduction of vertical velocity is scaled by the Kolmogorov velocity u_η: with this normalization, the change in vertical velocity due to radiation appears, in fact, stronger for heavier particles. As mentioned above, a smaller settling velocity in the high loading case limits the drag force exerted by the particles, which would otherwise greatly enhance the turbulent energy. These two effects of radiation, i.e. the generation of buoyant plumes and the hindering of particle settling, have opposite effects on the production of TKE. This explains the non-monotonic behavior reported in Figure 2.

In order to gain insight into the settling process, we investigate the probability density functions of the vertical component of the instantaneous particle velocity, w_p, for each case. These are reported in Figure 6, normalized by the nominal terminal velocity. w_p is taken as positive when upward. For the lighter particles ($\rho_p/\rho_o = 833$; Figure 6, left panel), the distributions show a marked increase in vertical velocity variance with increasing radiation level. This is the consequence of the higher turbulence level promoted by the radiation. For heavier particles, the change in variance is not monotonic with

increasing radiation, and follows the same trend as the turbulent kinetic energy, seen in Figure 2.

4. Conclusions

We have performed computations of inertial particles falling through homogeneous turbulence while heated by thermal radiation. In the considered optically thin regime, radiation is simply modeled as a constant heat flux input to each particle. Particles much smaller than the Kolmogorov scale are considered, in a Stokes number regime that produces strong preferential concentration. Both momentum and thermal coupling with the fluid are taken into account.

In the absence of radiation, particles with settling parameter $V_t/u_\eta \approx 1$ experience substantial increase of their settling velocity due to preferential sweeping of the turbulent eddies, as expected from previous studies. Heavier particles with $V_t/u_\eta > 1$ cause a significant augmentation of turbulent energy, and an increase in the vertical fluid velocity fluctuations with respect to the horizontal component. In the presence of radiation, buoyant plumes are shed from the heated particles, opposing their downward motion, and their settling velocity is reduced. The preferential sweeping mechanism breaks down: particles do not show the tendency to sample region of downward moving fluid.

For particles with $V_t/u_\eta \leq 1$, at the radiation intensity levels tested, turbulent kinetic energy is increased over all scales of the spectrum. The turbulence becomes strongly anisotropic, and the distribution of particle vertical velocities broadens greatly. For particles with $V_t/u_\eta > 1$, increasing radiation results in a non-monotonic variation of turbulent kinetic energy. This is due to the counteracting effects of the reduced settling velocity and the buoyancy-driven turbulence production.

Acknowledgments

The authors acknowledge use of computational resources from the Certainty cluster awarded by the National Science Foundation to CTR.

REFERENCES

Aliseda, A., Cartellier, A., Hainaux, F. & Lasheras, J. 2002 Effect of preferential concentration on the settling velocity of heavy particles in homogeneous isotropic turbulence. *J. Fluid Mech.* **468**, 77–105.

Balachandar, S. & Eaton, J. 2010 Turbulent dispersed multiphase flow. *Annu. Rev. Fluid Mech.* **42**, 111–133.

Bec, J., Biferale, L., Boffetta, G., Celani, A., Cencini, M., Lanotte, A., Musacchio, S. & Toschi, F. 2006 Acceleration statistics of heavy particles in turbulence. *J. Fluid Mech.* **550**, 349–358.

Boivin, M., Simonin, O. & Squires, K. 1998 Direct numerical simulation of turbulence modulation by particles in isotropic turbulence. *J. Fluid Mech.* **375**.

Bosse, T., Kleiser, L., Hartel, C. & Meiburg, E. 2005 Numerical simulation of finite reynolds number suspension drops settling under gravity. *Phys. Fluids* **17**, 037101.

Bosse, T. L. K. & Meiburg, E. 2006 Small particles in homogeneous turbulence: Settling velocity enhancement by two-way coupling. *Phys. Fluids* **18**, 027102.

Bunner, B. & Tryggvason, G. 2002 Dynamics of homogeneous bubbly flows part 1. rise velocity and microstructure of the bubbles. *J. Fluid. Mech* **466**, 17–52.

Capecelatro, J., Desjardins, O. & Fox, R. 2014 Numerical study of collisional particle dynamics in cluster-induced turbulence. *J. Fluid Mech.* **747**.

Dejoan, A. & Monchaux, R. 2013 Preferential concentration and settling of heavy particles in homogeneous turbulence. *Phys. Fluids* **25**, 013301.

Eaton, J. & Fessler, J. 1994 Preferential concentration of particles by turbulence. *Int. J. Multiphase Flow* **20**, 169–209.

Elghobashi, S. & Truesdell, G. 1993 On the two-way interaction between homogeneous turbulence and dispersed solid particles. 1: Turbulence modification. *Phys. Fluids* **5**, 1790–1801.

Ferrante, A. & Elghobashi, S. 2003 On the physical mechanisms of two-way coupling in particle-laden isotropic turbulence. *Phys. Fluids* **15**, 315.

Maxey, M. & Patel, B. 2001 Localized force representations for particles sedimenting in stokes flow. *Int. J. Multiphase Flow* **27**, 1603–1626.

Poelma, C., Westerweel, J. & Ooms, G. 2007 Particle-fluid interactions in grid-generated turbulence. *J. Fluid Mech.* **589**, 315–351.

Rosales, C. & Meneveau, C. 2005 Linear forcing in numerical simulations of isotropic turbulence: Physical space implementations and convergence properties. *Phys. Fluids* **17**, 095106.

Squires, K. & Eaton, J. 1990 Particle response and turbulence modification in isotropic turbulence. *Phys. Fluids* **2**, 1191.

Sundaram, S. & Collins, L. 1997 Collision statistics in an isotropic particle-laden turbulent suspension. part 1. direct numerical simulations. *J. Fluid Mech.* **335**, 75–109.

Wang, L. & Maxey, M. 1993 Settling velocity and concentration distribution of heavy particles in homogeneous isotropic turbulence. *J. Fluid Mech.* **371**, 179–205.

Yang, C. & Lei, U. 1998 The role of the turbulent scales in the settling velocity of heavy particles in homogeneous isotropic turbulence. *J. Fluid Mech.* **371**, 179–205.

Yang, T. & Shy, S. 2005 Two-way interaction between solid particles and homogeneous air turbulence: particle settling rate and turbulence modification measurements. *J. Fluid Mech.* **526**, 171–216.

Zamansky, R., Coletti, F., Massot, M. & Mani, A. 2014 Radiation induces turbulence in particle-laden fluids. *Phys. Fluids* **26**, 071701.